Molecular Spin-Flip Loss and a Dual Quadrupole Trap

David Reens,* Hao Wu, Tim Langen,† and Jun Ye
JILA, National Institute of Standards and Technology and the University of Colorado
Department of Physics, University of Colorado, Boulder, Colorado 80309-0440, USA
(Dated: April 18, 2017)

Doubly dipolar molecules exhibit complex internal spin-dynamics in combined electric and magnetic fields. Near magnetic trap minima, these spin-dynamics lead to enhancements in Majorana spin-flip transitions by many orders of magnitude relative to atoms, and are thus an important obstacle for progress in molecule trapping and cooling. The effect is strongest for Hund's case (a) states but is significant for Hund's case (b) as well. We study these internal spin-dynamics with OH molecules and devise a trap geometry where spin-flip loss can be tuned from over 200 s^{-1} to complete removal with only a weak external bias coil and with no sacrifice of trap strength.

The ultracold regime extends toward molecules on many fronts [1]. KRb molecules have reached lattice quantum degeneracy [2] and other bialkalis continue to progress [3, 4]. Creative and carefully engineered laser cooling strategies are tackling certain nearly vibrationally diagonal molecules [5–9]. A diverse array of alternative strategies have succeeded to greater or lesser extents on other molecules [10–15]. All of these molecules will require secondary strategies like evaporation or sympathetic cooling to make further gains in phase space density. They also may face a particular challenge: spin flip loss near the zero of a magnetic trap, but dramatically enhanced for many doubly dipolar molecules due to their internal spin dynamics in mixed electric and magnetic fields.

The knowledge of spin flips or Majorana hops as an eventual trap lifetime limit predates the very first magnetic trapping of neutrals [16]. Spin flips were directly observed near 10 μK and overcome in the TOP trap [17], and soon later with a plugged dipole trap [18], famously enabling the first Bose-Einstein condensates. In our earlier investigations, we observed trap loss with applied electric field [19]. This trap loss occurred for sub-states of OH's $^2\Pi_{3/2}$ ground state manifold other than the most well-trapped one (Fig. 1, panel (d)), and was attributable to avoided crossings that open at non-zero magnetic fields between levels of opposite parity. We have now identified trap loss at zero magnetic field with the application of electric field that afflicts even the most well-trapped substate although it lacks any such crossings. We first suspected this during experiments in our previous trap geometry, a 3D permanent magnet quadrupole trap with homogeneous electric field [21], but it was difficult to disentangle it from competing effects. Our new trap geometry addresses this, but we use our previous geometry as our starting point to explain the internal spin-dynamics that lead to the enhanced loss.

These internal spin-dynamics are subtle; it has taken a concentrated several year effort to elucidate the effect with conclusive experimental evidence as reported here. The effect has also eluded three previous investigations of note: In [22] the analogues of atomic spin-flip loss for molecules in mixed fields were studied, and a magnetic quadrupole trap for OH molecules with superposed electric field was specifically addressed. It was concluded that no significant loss enhancement due to electric field would be evident. While this is true for the approximate $^2\Pi_{1/2}$ Hamiltonian used in that study, it is not true for the actual $^2\Pi_{3/2}$ ground state of OH. In [21] E-fields were applied in our magnetic quadrupole trap to study E-field induced collisions. Although an initial suspicion existed of the effect we describe, efforts to deconvolve it underestimated its magnitude [23] Finally, in [24] it was correctly noted that Hund's case (a) molecules maintain a quantization axis in mixed fields. In fact the states of

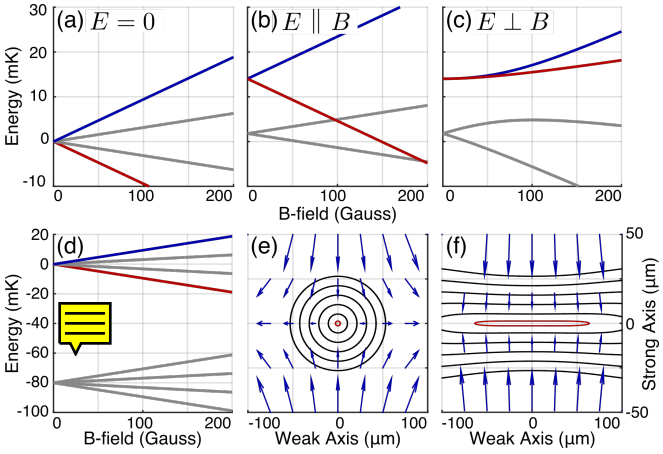

FIG. 1. (a) Four Zeeman split lines in OH's $J = 3/2$ ground manifold, with the well-trapped state in blue and it's spin-flip partner in red. (b) Again with $E = 150$V/cm, and $E \| B$. (c) Again with $E \perp B$. Note vastly reduced red-blue splitting. Other angles in appendix of [21]. (d) The opposite parity manifold of electrically strong field seeking substates sits 80 mK below, this is the lambda doublet splitting Δ. (e) Energy splitting contours every 2 mK near the zero of a magnetic quadrupole trap with 2 T/cm gradient [19]. B-field vectors in blue. (f) Again with $E = 150$ V/cm. Note drastic widening of lowest contour (red). Vector direction gives the effective quantization axis of the trapped state, $\mu_B B \pm d_E E$ above (below) the horizontal centerline. Vector magnitude gives potential energy relative to trap center.

the molecule align with one of two quantization axes- either the vector sum or the vector difference of the dipole moment weighted electric and magnetic fields. It was asserted that this would maintain quantization near the zero of a quadrupole trap and avoid spin-flip loss. As we will now explain, quantization is indeed maintained, but spin-flip loss is enhanced:

With only magnetic field, a molecule remains trapped insofar as it adiabatically follows the field direction. Near the trap center, the direction changes most rapidly, enabling loss. When electric field is added, it dominates in the trap center where the magnetic field is weakest. Quantization is maintained but the quantization axis does not rotate with the magnetic field as it needs to. Further away from the trap center the molecule is then magnetically strong field seeking and is lost. The molecule ought to have switched from the vector sum quantization axis to the vector difference quantization axis, so as to remain doubly weak field seeking despite the change in relative orientation of the fields. To be more precise, we define the relative orientation of the fields as the sign of $\phi = \vec{E} \cdot \vec{B}$. When ϕ is negative (positive), the doubly trapped state must have the vector difference (sum) quantization axis, so that an increase in magnitude of either field increases it's energy. Orientation changes whenever ϕ changes sign, which occurs in a 2D region given by $\phi = 0$, i.e. $E \perp B$. This region must be 2D, since it is a contour level of the 3D scalar valued function ϕ.

We can also understand this effect in terms of the energy splitting between the well trapped substate and it's spin-flip partner, since this splitting acts as a barrier to spin-flips. The preceding quantization axis discussion suggests that spin-flips occur when crossing the $\phi = 0$ planar region, so we expect to find a correspondingly reduced energy splitting there. In Fig. 1, the energies of the well trapped state and its spin-flip partner are calculated by diagonalizing OH's $X^2\Pi_{3/2}$ ground state Hamiltonian verses B-field without E-field in panel (a), with fixed E-field and $E \| B$ so that ϕ is maximally nonzero in panel (b), and with fixed E-field and $\phi = 0$ in panel (c). Indeed, we find a striking reduction in energy splitting for a wide range of magnetic fields in panel (c) compared with panel (b). In fact, by series expanding the exact eigenenergies of OH, we find $H_{E\perp B}(B) \approx (\mu_B B)^3 \Delta^2/(d_E E)^4$, Δ the lambda doubling term. The Zeeman splitting is no longer linear, but cubic. This means that the splitting will be small in a much larger region close to $B = 0$ then otherwise.

This observation allows us to develop a scaling law for the loss enhancement in this geometry. For a given trap strength and sample temperature, there is a characteristic energy splitting κ below which spin-flips can occur, calculated from the Landau-Zener formula. In our case $\kappa = 5$ MHz. As shown in panel (e) of Fig. 1, E-field widens the κ valued energy contour near the trap zero, greatly increasing the flux through this region. Note also that the energy gradient near the loss region, which also contributes to the Landau-Zener hopping probability, remains nearly identical in the z-direction between panels (d) and (e). Solving for B when $H_{E\perp B}(B) = \kappa$ and dividing by the $E = 0$ case gives the flux enhancement factor $\nu = (d_E E/\sqrt{\kappa\Delta})^{8/3}$. So E-fields beyond $\sqrt{\kappa\Delta}/d_E$ lead to almost cubic enhancements in spin-flip loss. We can be more quantitative by integrating the velocity distribution and the flux through the plane, accounting for the velocity dependent Landau-Zener probability, Table. I. The spin-flip loss is negligible at 50 mK, but relevant at the 5 mK targeted during evaporation [25]. Those results will thus require reinterpretation considering this effect [26]. With the goal of μK temperatures and below, it is clear spin-flip loss must be addressed.

TABLE I. Enhancements and loss rates for OH. Evaporation E-field detailed in [25]. Spectroscopic E-field in [19]. Background loss is 2 s^{-1}, experiment length 100 ms.

E (V/cm)	45 mK		5 mK		Purpose
	ν	$\Gamma\,(s^{-1})$	ν	$\Gamma\,(s^{-1})$	
0	1	0.02	1	1.3	No Field
300	5	0.1	9	11	Evaporation
550	17	0.3	40	50	Spectroscopy
3000	1000	19	1600	2000	Polarizing

For Hund's case (a) states more generally, the Zeeman splitting when $E \perp B$ is reduced from linear to order $2J$, according to several test Hamiltonians we have diagonalized. This also agrees with the intuition that when $\mu_B B << d_E E$ and $E \perp B$, the magnetic field must un-do the electric field's coupling of opposite m_J number states, a task of order $m_J - (-m_J) = 2J$. Only $J = 1/2$ states remain linear, but their vanishing g-factor renders them untrappable already. For Hund's case (b) the enhanced loss region is restricted to the trap energy regime where γ the spin-rotation coupling dominates. In this regime the state is effectively Hund's case (a). This can still be very significant, for example $\gamma = 75$ MHz for SrF [27]. In preliminary investigations for Hund's case (b) molecules, which essentially consist of reproducing panels (a)-(c) of Fig. 1 for different Hamiltonians, we find large spin-flip loss enhancements for SrF's v=0, N=1 magnetically trappable substates. Some Hund's case (b) molecular states such as YO's v=0, N=1 manifold have a protected substate with $m_F = 0$ and thus no hopping partner in the spin-rotation coupling regime that is nonetheless energetically separated from other state-crossings by the lamb-shift. This state is less strongly trappable due to the same $m_F = 0$ feature, but is fully spin-flip immune.

We can generalize to arbitrary geometries and consider methods to avoid the loss using a simple strategy: avoid $\mu_B B < d_E E$ where $E \perp B$. One way to achieve this is to trap with E-field and superpose B-field. The lambda

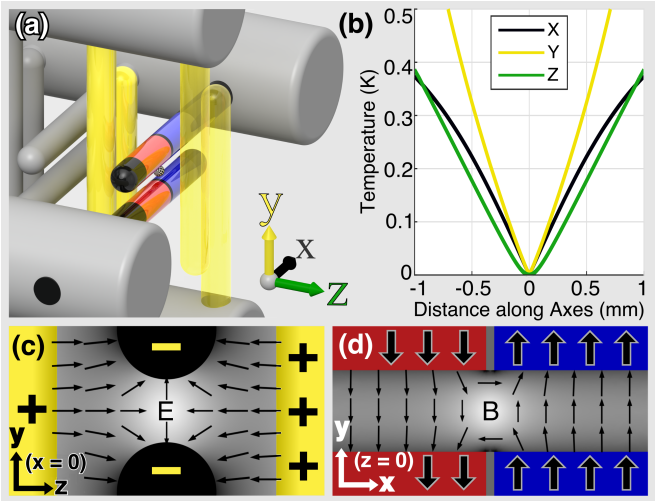

FIG. 2. (a) The trap consists of the last 6 pins of a Stark decelerator. The trap center is directly between the second to last pin pair. These pins have two magnetized domains each. The blue domains are magnetized along $+\hat{y}$, the red along $-\hat{y}$. These pins are grounded, while those in yellow are positively charged. OH is decelerated as in [20], except the slowing reaches almost zero velocity at the trap center. (b) Trap energy along axes. $B' = 5$ T/cm and $E' = 100$ kV/cm^2. Trap frequencies $\nu_x = 3$ kHz, $\nu_y = 5$ kHz, and $\nu_z = 4$ kHz. Pin-pairs are spaced 2 mm, which sets the maximum trap width in the y direction. (c) The electric 2D quadrupole in the $x = 0$ plane. The magnetic pins intersect this plane and are shown as black circles. The other pins don't actually intersect this plane, but are projected onto it as yellow rectangles. (d) The magnetic 2D quadrupole in the $z = 0$ plane.

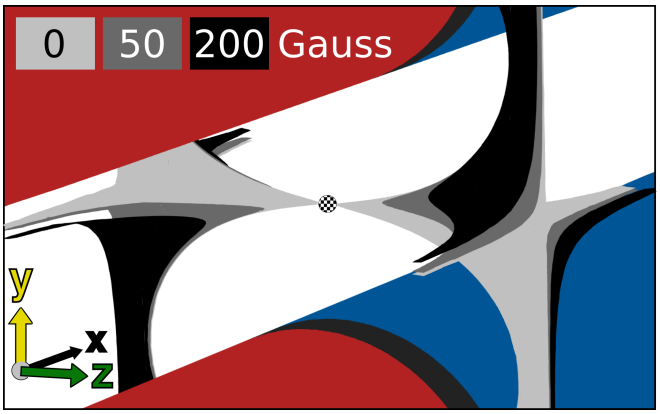

FIG. 3. Surfaces where spin-flips can occur for several values of B_{coil}. These surfaces are subsets of those where $E \perp B$, shown only where $\mu_B B$ is small enough relative to $d_E E$ to allow spin-flips.

doublet prevents flips in this configuration, but it does round the trap minimum consider Another option is to trap with both fields and keep zeros overlapped. This was once realized for OH with a superposed magnetic quadrupole and electric hexapole [28]. Such a scheme prevents spin-flip loss enhancement, but does not remove it entirely. It is also susceptible to misalignment induced loss enhancement. Another possibility is to use one field only. While this avoids spin-flip loss enhancement, any experiment which aims to make use of the doubly dipolar nature of molecules cannot accept this compromise.

We opt for a geometry that is distinct from these options: a pair of 2D quadrupole traps, one magnetic and the other electric, with orthogonal centerlines. We achieve these fields in a geometry that matches our Stark decelerator [12], as shown in Fig. 2. This approach is similar to the Ioffe-Pritchard strategy [29], where a 2D magnetic quadrupole is combined with an axial dipole trap. Axial and radial trapping interfere, resulting in significantly lower trap depths than the 3D quadrupole. We thwart this interference by using electric field for the third direction. Our geometry has $E \perp B$ along both the xz and yz planes, with $\mu_B B < d_E E$ in a large cylinder surrounding the z-axis. However, by adding magnetic field $\vec{B} = B_{\text{coil}}\hat{z}$ along the centerline of the magnetic quadrupole with an external bias coil, a fully tunable scenario emerges.

Adding B_{coil} only slightly rounds the magnetic trapping potential, but it morphs the $E \perp B$ surface from a pair of planes into a hyperbolic sheet, pushing it away from the z-axis where the magnetic field is smallest. This means that small magnitudes of B_{coil} are sufficient to avoid $\mu_B B < d_E E$ where $E \perp B$. In Fig. 3, the surfaces where $E \perp B$ for several B_{coil} magnitudes are shown wherever the splitting there is below the hopping threshold κ. Note how B_{coil} tunes the proximity of the loss regions to the trap center. The loss regions are always visible, but they are tuned so far away that molecules accessing them have already escaped the trap. The striking difference in molecule trap lifetime with and without B_{coil} can be seen in Fig. 4, panel (a).

As a further confirmation of our $E \perp B$ and $\mu_B B < d_E E$ model of the loss, we translate our magnetic pins along the $\hat{x}$ direction in their mounts to alter the surface where $E \perp B$ and compare experimental data against our expectations. The data are shown in Fig. 4, panel (b). Qualitatively, this translation serves to disrupt the otherwise perfectly 2D magnetic quadrupole by adding a small trapping field $\vec{B} \propto B' z\hat{z}$ along the z-axis. This means that B_{coil} no longer directly tunes the magnetic field magnitude along the z-axis. Instead, B_{coil} must first overcome the slight trapping field along the z-axis, translating a point of zero field along the z axis and eventually out of the trap. The point of zero magnetic field has $\mu_B B < d_E E$ and lies on the $\phi = \vec{E} \cdot \vec{B} = 0$ surface by definition, leading to strong loss unless it is aligned with the trap center, where E is also zero. This means that without any bias field, the loss should actually be a local minimum; as the field is increased in either direction the loss should first worsen and then improve when the zero leaves the trap. This qualitative explanation correctly

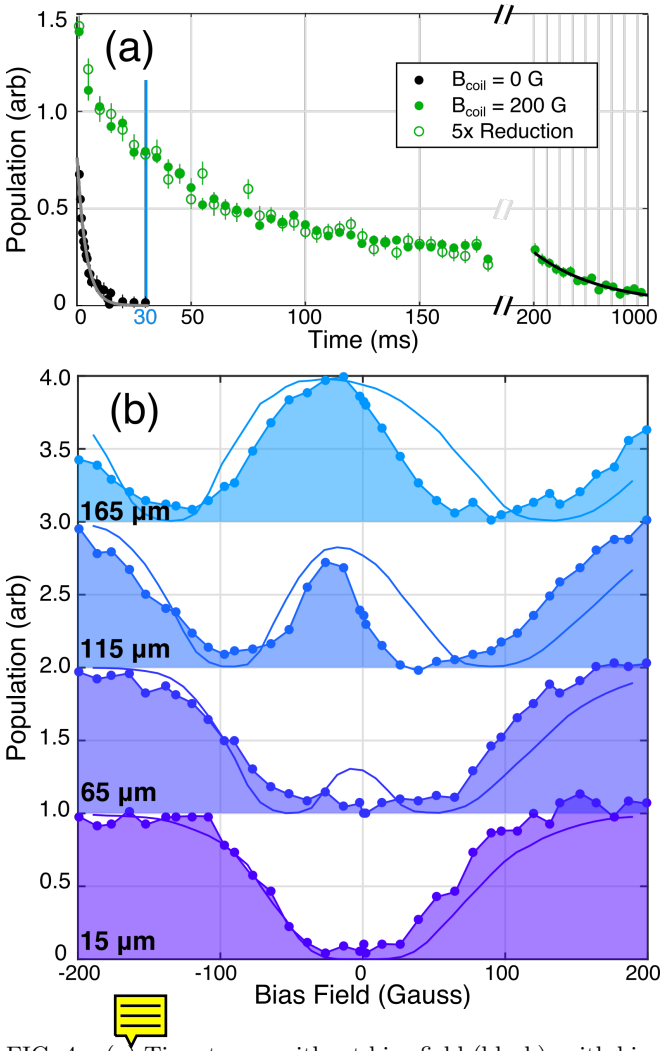

FIG. 4. (a) Time traces without bias field (black), with bias field (green dots), and with modulated density (green circles). A one body fit (gray) to the data without bias field yields a 200 s^{-1} loss rate. A one body fit (black) to the long time bias field data yields a 2 s^{-1} loss rate, in agreement with our background gas pressure. (b) At the fixed time 30ms, population is shown as a function of both pin translation and bias field.

predicts the observed double well structure.

Quantitatively, we fit the family of curves shown in Fig. 4(b) by performing an integration of molecule flux weighted by Landau-Zener probability and Maxwell-Boltzmann population density over the strangely twisted surfaces where $E \perp B$ for each $B_{\rm coil}$ and pin offset. The computation is performed in COMSOL Multiphysics, with cloud temperature as the only free parameter [30]. The asymmetry of the curves about $B_{\rm coil} = 0$ comes from a slight shift of the electric quadrupole minimum caused by an intentional bending of the last pin pair to increase fluorescence collection along $\hat{z}$. The fitted temperature is in the $100 - 200$ mK range, larger than expected from our simulations, despite the known defocusing and reflection losses that accompany pulsed decelerators at low

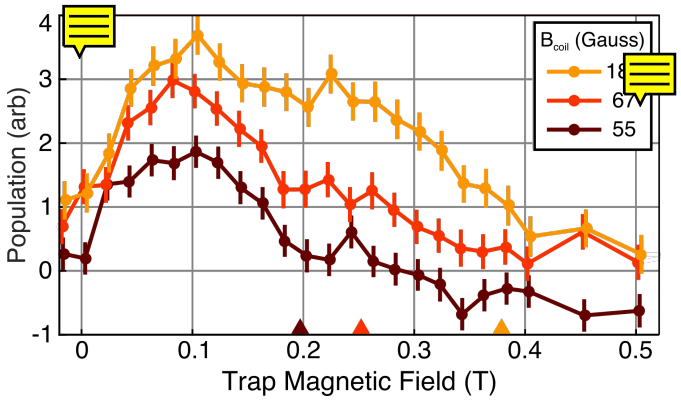

FIG. 5. Microwave Thermometry at different values of $B_{\rm coil}$. Increasing $B_{\rm coil}$ increases and shifts population as expected. The location of the lowest trap energy at which a molecule can access loss regions for a given $B_{\rm coil}$ is indicated with a correspondingly colored triangle on the magnetic field axis.

speeds [31]. This may be related to micro-discharges on the surfaces of the magnetic pins during the final deceleration pulse, since these pins are less well polished. This could be overcome with various polishing strategies.

We further confirm the consistency of our model of the loss using microwave spectroscopy as performed as in our previous work [25]. Instead of using a bias tee setup, we use a microwave probe to excite free space modes of our vacuum chamber in a near field manner. The results are shown in Fig. 5. It is seen that increasing $B_{\rm coil}$ increases population first at low fields and then at higher fields. This is consistent with our calculations of the location of the loss as presented in Fig. 3. In order to perform this spectroscopy, the trapping electric fields are switched off immediately prior to Zeeman specific microwave transfer pulses. Thus the results reflect the Zeeman potential energy only, which in the ensemble average tracks potential energy but is not directly proportional. Nonetheless, the shift in population center is clear and in agreement with our expectation.

In the case of lowest applied magnetic field in Fig. 5, a negative going signal is observed. This indicates a build-up in the opposite parity weak electric field seeking state. Although the spin-flips we have discussed do not connect states of opposite parity, other avoided crossings amongst the ground state manifold result in the spin-flipped molecules remaining very weakly trapped in a secondary state with opposite parity character in some regions.

With loss removed, we observe the green-dotted trend in Fig. 4(a). The decay rate decreases with population over the first 200 ms, a timescale that is long compared with trap frequency and thus suggestive of a collisional process. To test this, we reduce the molecule number five-fold with a technique that ought to be phase-space blind so as to reduce the molecule density. We do this with microwaves as before, but coupling electrically weak and

strong field seekers during the first half of deceleration. Spatial inhomogeneities on the order of the cloud size are unlikely given the 15 cm microwave wavelength, but any that exist are remixed during the remaining deceleration. The trend remains similar with this density-modulation, suggesting that single-particle physics is chiefly responsible. This discrepancy relative to our previous work is attributable to our warmer initial temperature. We hope soon to implement several density increasing measures and return to the collisional regime. The slowly varying but single-body decay rate could be related to the existence of high energy chaotic orbits with long escape times, as seen in other exotically shaped trapping potentials [32].

Our dual quadrupole trap decisively overcomes molecule enhanced spin-flip loss by tuning it from an overwhelming rate to complete removal. Our explanation of the loss provides detailed predictions of how its location and magnitude ought to scale with bias field and trap alignment, which we have experimentally verified. Our results correct existing predictions about molecular spin-flips in mixed fields and we provide a consistent framework that explains this based on internal spin-dynamics. We have devised a viable trapping geometry in which spin-flip loss is fully mitigated without trap-depth sacrifice, paving the way toward further improvements in molecule trapping and cooling.

We acknowledge the Gordon and Betty Moore Foundation, the ARO-MURI, JILA PFC, and NIST for their financial support. T.L. acknowledges support by the Alexander von Humboldt Foundation through a Feodor Lynen Fellowship. We thank J.L. Bohn and S.Y.T. van de Meerakker for helpful discussions. We thank Goulven Quéméner for his continued involvement.

D.R. and H.W. contributed equally: D.R. in writing and trap design, H.W. in experiment execution.

* dave.reens@colorado.edu
† Present Address: 5. Physikalisches Institut and Center for Integrated Quantum Science and Technology (IQST), Universität Stuttgart, Pfaffenwaldring 57, 70569 Stuttgart, Germany

[1] L. D. Carr, D. DeMille, R. V. Krems, and J. Ye, New Journal of Physics **11**, 055049 (2009).
[2] S. A. Moses, J. P. Covey, M. T. Miecnikowski, B. Yan, B. Gadway, J. Ye, and D. S. Jin, Science **350**, 659 (2015).
[3] T. Takekoshi, L. Reichsöllner, A. Schindewolf, J. M. Hutson, C. R. Le Sueur, O. Dulieu, F. Ferlaino, R. Grimm, and H.-C. Nägerl, Physical Review Letters **113**, 205301 (2014).
[4] J. W. Park, S. A. Will, and M. W. Zwierlein, Physical Review Letters **114**, 205302 (2015).
[5] M. T. Hummon, M. Yeo, B. K. Stuhl, A. L. Collopy, Y. Xia, and J. Ye, Physical Review Letters **110**, 143001 (2013).
[6] J. F. Barry, D. J. McCarron, E. B. Norrgard, M. H. Steinecker, and D. DeMille, Nature **512**, 286 (2014).
[7] V. Zhelyazkova, A. Cournol, T. E. Wall, A. Matsushima, J. J. Hudson, E. A. Hinds, M. R. Tarbutt, and B. E. Sauer, Physical Review A **89**, 053416 (2014).
[8] M. H. Steinecker, D. J. McCarron, Y. Zhu, and D. DeMille, ChemPhysChem **17**, 3664 (2016).
[9] B. Hemmerling, E. Chae, A. Ravi, L. Anderegg, G. K. Drayna, N. R. Hutzler, A. L. Collopy, J. Ye, W. Ketterle, and J. M. Doyle, Journal of Physics B: Atomic, Molecular and Optical Physics **49**, 174001 (2016).
[10] J. M. Doyle, J. D. Weinstein, R. DeCarvalho, T. Guillet, and B. Friedrich, Nature **395**, 148 (1998).
[11] H. L. Bethlem, G. Berden, and G. Meijer, Physical Review Letters **83**, 1558 (1999).
[12] J. R. Bochinski, E. R. Hudson, H. J. Lewandowski, G. Meijer, and J. Ye, Physical Review Letters **91**, 243001 (2003).
[13] E. Narevicius, A. Libson, C. G. Parthey, I. Chavez, J. Narevicius, U. Even, and M. G. Raizen, Physical Review Letters **100**, 093003 (2008).
[14] A. Wiederkehr, H. Schmutz, M. Motsch, and F. Merkt, Molecular Physics **110**, 1807 (2012).
[15] A. Prehn, M. Ibrügger, R. Glöckner, G. Rempe, and M. Zeppenfeld, Physical Review Letters **116**, 063005 (2016).
[16] A. L. Migdall, J. V. Prodan, W. D. Phillips, T. H. Bergeman, and H. J. Metcalf, Physical Review Letters **54**, 2596 (1985).
[17] W. Petrich, M. H. Anderson, J. R. Ensher, and E. A. Cornell, Physical Review Letters **74**, 3352 (1995).
[18] K. B. Davis, M. O. Mewes, M. R. Andrews, N. J. van Druten, D. S. Durfee, D. M. Kurn, and W. Ketterle, Physical Review Letters **75**, 3969 (1995).
[19] B. K. Stuhl, M. Yeo, B. C. Sawyer, M. T. Hummon, and J. Ye, Physical Review A **85**, 033427 (2012).
[20] B. C. Sawyer, B. K. Stuhl, D. Wang, M. Yeo, and J. Ye, Physical Review Letters **101**, 203203 (2008).
[21] B. K. Stuhl, M. Yeo, M. T. Hummon, and J. Ye, Molecular Physics **111**, 1798 (2013).
[22] M. Lara, B. L. Lev, and J. L. Bohn, Physical Review A **78**, 033433 (2008).
[23] Although the underestimate was only by a factor of three, it is unclear how much of the collisional effect described in [21] remains. This will be the subject of further investigation.
[24] J. L. Bohn and G. Quéméner, Molecular Physics **111**, 1931 (2013).
[25] B. K. Stuhl, M. T. Hummon, M. Yeo, G. Quéméner, J. L. Bohn, and J. Ye, Nature **492**, 396 (2012).
[26] Spin-flip loss would have interfered with evaporation before 5 mK was attained. Some phase space compression does seem to have occurred at 20 mK.
[27] G. Quéméner and J. L. Bohn, Physical Review A - Atomic, Molecular, and Optical Physics **93**, 1 (2016).
[28] B. C. Sawyer, B. L. Lev, E. R. Hudson, B. K. Stuhl, M. Lara, J. L. Bohn, and J. Ye, Physical Review Letters **98**, 1 (2007).
[29] D. E. Pritchard, Physical Review Letters **51**, 1336 (1983).
[30] Soure code: https://github.com/dreens/spin-flip-integration/.
[31] B. C. Sawyer, B. K. Stuhl, B. L. Lev, J. Ye, and E. R. Hudson, European Physical Journal D **48**, 197 (2008).
[32] R. González-Férez, M. Iñarrea, J. P. Salas, and

P. Schmelcher, Physical Review E **90**, 062919 (2014).